Physical and optical traits of tellurite glass: effect of bimetallic TiO_2/Au nanoparticles

A. M. Machinin, A. Awang*, C. F. Pien
Industrial Physics Programme, Faculty of Science and Natural Resources, Universiti Malaysia Sabah, 88400 Kota Kinabalu, Sabah, Malaysia

The dependence of TiO_2/Au concentrations on the physical and optical properties of glass was investigated thoroughly. Variations in density, molar volume, molar refraction, refractive index, and polarizability with varying TiO_2/Au contents were affected by the formation of non-bridging oxygen. The formation of big islands in the atomic force microscopy image signifies the growth of nanoparticles. The decrement in band gap manifests alteration in the glass network mainly the local field around the Er^{3+} ions. The rise in Urbach energy illustrates disorder in the glass. The beneficial features of the current glass composition may be useful for photonic devices.

(Received March 8, 2023; Accepted June 7, 2023)

Keywords: Glass, Metallic nanoparticles, Non-bridging oxygen, Band gap, Urbach energy

1. Introduction

Glasses exhibit several prevalent inherent properties such as good mechanical strength, high transparency, absence of metal-ligand interaction, and facile production in desired sizes and shapes. These features enable glass to be used as a host for encapsulating both metal nanocrystals and rare earth ions [1]. Among various methods to produce metal-glass nanocomposites, the melt quench method is highly decisive to integrate metal NPs in a congruent manner in the glass network under the specific condition of low concentrations of metal NPs [2]. The integration of multi-metallic NPs in the form of core-shell or alloy structures emerges as appealing materials due to their significant features of composition-dependent optical, catalytic, electronic, and magnetic properties that noticeably possess different features from those of their monometallic counterparts [3]. Further, noble metal NPs such as Ag, Au, and Cu have represented advantages due to their significant optical properties of Surface Plasmon Resonance (SPR) which display the resonance oscillation of the free electrons [2,4].

The collective oscillation of plasma of conduction electrons occurs when a considerable wavelength of light hits metallic NPs and leads to the emergence of various nonlinear mechanisms [2]. Though the manipulation of NPs with controlled shapes has become an integral component in the research field due to their specific geometries exerting remarkable physical and chemical properties on the final product [3]. This is because the optical properties of NPs in glasses are greatly affected by their shape, size, and dielectric constant of the neighboring medium [2]. The current study demonstrated the direct inclusion of bimetallic TiO_2 and Au NPs in the glass matrix. The lower concentration of Au NPs varied from 0.03 mol% to 0.20 mol% to evaluate the changes in the glass network that affects the physical and optical traits of glass.

2. Experimental details

2.1. Fabrication of glass

Table 1 shows a series of glasses with a nominal composition of $(70-x-y)TeO_2$–$20ZnO$–$9Na_2O$–$1Er_2O_3$–$(x)TiO_2$–$(y)Au$ where x = 0, 0.3 mol% and y = 0, 0.03, 0.05, 0.10, 0.15, 0.20

* Corresponding author: asmahani_awang@ums.edu.my
https://doi.org/10.15251/JOR.2023.193.321

mol% was prepared by employing a melt-quenching method. The raw materials were weighed by using an electronic balance. Each batch of glass has 15±0.001 grams of the total weight of constituent powders. The milling process was performed for a duration of 30 minutes to produce homogeneous powder mixing. Then, the powders were placed into a platinum crucible and kept in a muffle furnace Carbolite CWF with a temperature of 970 °C for 30 minutes. Then, the molten was transferred into a brass mold and subjected to an annealing process with a temperature of 300 °C for 3 hours and cooled down to room temperature for further characterization.

Table 1. Glass code and glass composition.

Glass Code	TeO_2 (mol%)	ZnO (mol%)	Na_2O (mol%)	Er_2O_3 (mol%)	TiO_2 (mol%)	Au (mol%)
TZNE	70	20	9	1	0	0
TZNETi	69.7	20	9	1	0.3	0
TZNETiAu0.03	69.67	20	9	1	0.3	0.03
TZNETiAu0.05	69.65	20	9	1	0.3	0.05
TZNETiAu0.10	69.60	20	9	1	0.3	0.10
TZNETiAu0.15	69.55	20	9	1	0.3	0.15
TZNETiAu0.20	69.50	20	9	1	0.3	0.20

2.2. Characterization of glass

2.2.1. Physical properties

The density of glass is evaluated by applying the Archimedes method (Analytical balance of specific density-PrecisaXT220A). Distilled water, ρ_x with a density of 1 g.cm^{-3} was used as the reference immersion liquid. The density (ρ) was calculated by [5]

$$\rho = \frac{W_a}{W_a - W_b}\rho_x \tag{1}$$

where W_a is the weight of the glass sample in air and W_b is the weight of the sample after immersion in distilled water. The molar volume (V_m) can be expressed as [6]

$$V_m = \frac{M}{\rho} \tag{2}$$

where M is the molecular weight of the sample. The refractive index (n) of glasses was determined by using [7]

$$\frac{n^2-1}{n^2+2} = 1 - \sqrt{\frac{E_{opt}}{20}} \tag{3}$$

where E_{opt} is the optical band gap of the glass. The molar refractivity (R_M) was assessed by [8]

$$R_M = \frac{n^2-1}{n^2+2}(V_m) \tag{4}$$

where V_m is the molar volume. The polarizability (α_e) of the glasses was evaluated by using an expression [9]

$$\frac{n^2-1}{n^2+2}(V_m) = \frac{4}{3}\pi N\alpha_e \tag{5}$$

where N is Avogadro's number. The absorption coefficients $\alpha(\lambda)$ were investigated by using [10]

$$\alpha = \frac{1}{d}\ln\left(\frac{I_0}{I}\right) \tag{6}$$

where d is the thickness of the sample, and $\ln(I_0/I)$ represents the absorbance.

2.2.2. Surface topography

The surface topography of the glass was probed using Bruker Multimode-8 atomic force microscopy (AFM) with a scan size of 10 μm. The images were explored using NanoScope software.

2.2.3. Band gap and Urbach energy

The absorption spectra were probed by utilizing Agilent Technologies Cary 60 UV-Vis spectrophotometer. The expression for $\alpha(\omega)$ as a function of photon energy for optical band gap was indicated by [6]

$$\alpha(\omega) = \frac{B(\hbar\omega - E_{opt})^n}{\hbar\omega} \quad (7)$$

where B is a constant, E_{opt} is the optical band gap, $\alpha(\omega)$ is the absorption coefficient at an angular frequency of $\omega = 2\pi\nu$, $\hbar$ is the Planck constant divided by 2π and n is the index with a value of 0.5, 1.5, 2, and 3 susceptible to the characteristic of electronic transitions that is responsible for the absorption. Urbach energy indicates the extent of the exponential tail of the absorption edge can be expressed as [6]

$$\alpha(\omega) = B\exp\left(\frac{\hbar\omega}{E_{tail}}\right) \quad (8)$$

where E_{tail} is the width of band tails of electron states.

3. Results and discussion

3.1. Physical properties

Figure 1a shows the density of glass with the inclusion of different concentrations of TiO_2 and Au NPs. The density lies in the range of 5.166 – 5.200 g.cm^{-3}. The first incorporation of TiO_2 NPs causes a decrease in the density of glass from 5.200 g.cm^{-3} to 5.166 g.cm^{-3} manifests an increasing number of non-bridging oxygen (NBO) in the glass network [8]. The addition of 0.03 mol% Au NPs (TZNETiAu0.03 glass) shows a slight increment in the density from 5.166 g.cm^{-3} to 5.189 g.cm^{-3}. The increase in the density of glass implies the escalation in the number of bridging oxygen (BO) [8]. Nonetheless, further inclusion of Au NPs causes a slight decrement in the density from 5.188 g.cm^{-3} to 5.183 g.cm^{-3}. The incorporation of higher Au content leads to the increasing number of NBO in the network structure which consequently decreases the density of glass.

Figure 1b illustrates the molar volume and molar refraction of glass. The molar volume lies in the range of 26.423 – 26.549 cm^3.mol^{-1}. The molar volume is affected by the density and molecular weight of the glass [11]. The first incorporation of TiO_2 NPs causes an expansion in the molar volume from 26.423 cm^3.mol^{-1} to 26.549 cm^3.mol^{-1} implying the elongation of the bonds within the network [8]. Further, the addition of 0.03 mol% Au NPs (TZNETiAu0.03 glass) shows a slight decrement in the molar volume from 26.549 cm^3.mol^{-1} to 26.434 cm^3.mol^{-1} manifesting the reduction of the bond's length [8]. Initially, Au NPs occupy the interstitial and voids [12]. However, increasing the Au content from 0.05 mol% to 0.20 mol% elevates the molar volume from 26.440 cm^3.mol^{-1} to 26.477 cm^3.mol^{-1} reflecting the expansion in volume to accommodate a higher number of Au NPs and leads to the reduction in density [12]. In another study, the expansion in the molar volume was associated with the generation of NBO that breaks the bond and uplifts the number of spaces in the network [13] that produce a less compact vitreous network [14]. The molar refraction lies in the range of 15.836 – 15.954 cm^3. The first incorporation of TiO_2 NPs causes an increase in the molar refraction from 15.836 cm^3 to 15.954 cm^3. In general, molar refraction and refractive index is affected by the polarizability of the material. The outer electrons are more polarized, leading to a greater value of the refractive index and molar refraction. The substitution of TiO_2 into TeO_2 stimulates the generation of NBO with higher ionic character and lesser bond energies. NBO bonds possess greater polarizability and cation refractions [15]. The introduction of 0.03 mol% Au NPs depicts a decrement in the molar refraction. However, the

inclusion of Au content beyond 0.30 mol% shows substantial enhancement in molar refraction manifesting an increasing number of NBO in the glass system.

Figure 1c represents the refractive index and polarizability of glass. The refractive index lies in the range of 2.343 – 2.349. The first inclusion of TiO_2 NPs increases the refractive index from 2.343 to 2.349. The incorporation of TiO_2 NPs increases the refractive index because of the generation of more Ti^{4+} ions in the glass networks. Subsequently, glass becomes more compact due to the increasing number of NBOs [16]. According to Elisa et al. [14], ionic bonding manifests a greater polarizability of the NBO as compared to the covalent bonding of the BO atoms. In NBO, there is a distortion of the outer electron shell in ligand fields. Therefore, the elevation in the number of NBO atoms raises the refractive index value. However, the incorporation of Au NPs causes a decrement in the refractive index of glass. The refractive index was associated with the molar volume. Reduction in the molar volume leads to the depletion of electron clouds which cannot be simply distorted and lowers the polarizability of the glass. This distortion produces dispersion forces in which lower dispersion results in lower bending or refraction of the light in the material. Consequently, there is a reduction in the refractive index [8].

The polarizability of glass lies in the range of 6.278×10^{-24} – 6.325×10^{-24} cm^3. The first introduction of TiO_2 NPs increases the polarizability from 6.278×10^{-24} cm^3 to 6.325×10^{-24} cm^3 due to the contribution of the lone pair electrons of the NBOs [17]. The incorporation of Au NPs with a concentration of 0.03 mol% causes a decrease in the polarizability of glass due to decreasing number of NBO. The number of BO with low polarizability is larger than the number of NBO with high polarizability leading TZNETiAu0.03 glass to be less polarized [18]. Though, the incorporation of Au NPs with a concentration beyond 0.03 mol% elevates the number of NBO and causes substantial enhancement in the polarizability of glass. NBO possesses a high tendency to polarize contrasted with BO.

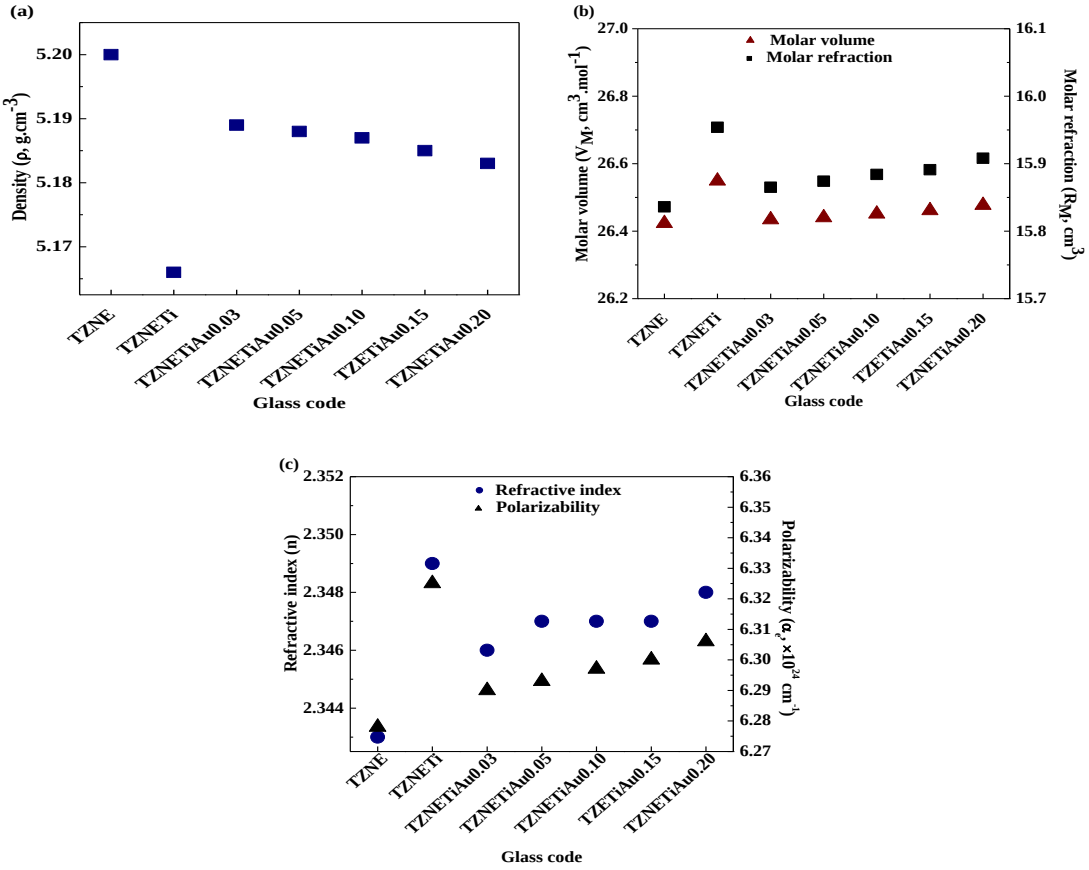

Fig. 1. Variations in the (a) density (b) molar volume and molar refraction (c) refractive index and polarizability.

Therefore, the glasses tend to be more polarized since the number of BO that possesses lower polarizability is smaller than the number of NBOs that possess high polarizability. Variation in density, molar volume, molar refraction, refractive index, and polarizability of glass is summarized in Table 2.

Table 2. Physical properties of glass.

Physical properties	Glass code						
	TZNE	TZNETi	TZNETiAu0.03	TZNETiAu0.05	TZNETiAu0.10	TZNETiAu0.15	TZNETiAu0.20
Molecular mass, M_{av} ($g.mol^{-1}$)	137.398	137.159	137.170	137.177	137.196	137.214	137.234
Density, ρ ($g.cm^{-3}$)	5.200	5.166	5.189	5.188	5.187	5.185	5.183
Molar volume, V_M ($cm^3.mol^{-1}$)	26.423	26.549	26.434	26.440	26.451	26.461	26.477
Molar refractions, R_M (cm^3)	15.836	15.954	15.865	15.874	15.884	15.891	15.908
Refractive index, n	2.343	2.349	2.346	2.347	2.347	2.347	2.348
Polarizability, α_e ($\times 10^{-24}$ cm^3)	6.278	6.325	6.290	6.293	6.297	6.300	6.306

3.2. Surface topography

Figures 2a and 2b illustrate the three-dimensional AFM images of TZNE glass and TZNETiAu0.20 glass with a surface roughness in the range of 5.45 – 8.70 nm. The AFM image of TZNE glass shows the distribution of small and discrete islands. Meanwhile, the AFM image of TZNETiAu0.20 glass shows the distribution of big islands due to the consolidation of small islands in the adjacent area. The formation of bigger islands represents the growth of TiO_2/Au NPs following the coalescence process [19].

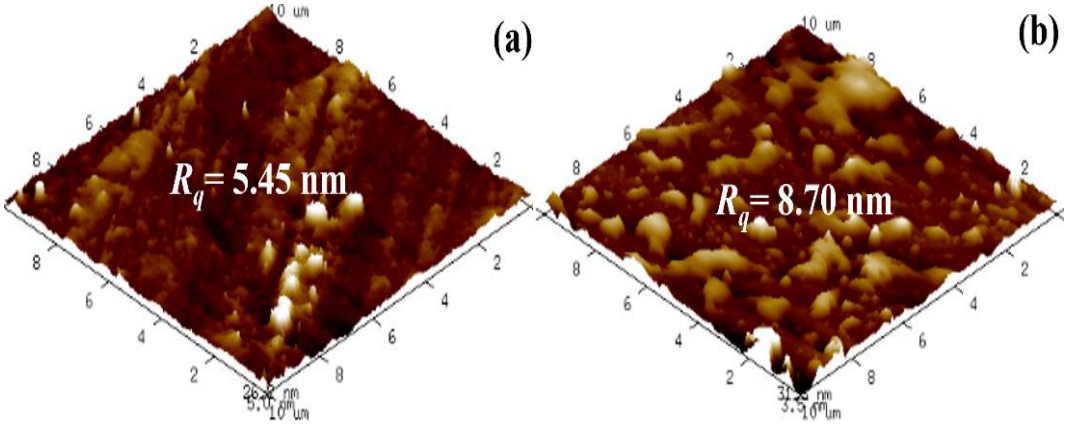

Fig. 2. AFM image of (a) TZNE glass (b) TZNETiAu0.20 glass.

3.3. Optical bandgap and Urbach energy

Figure 3a illustrates the UV-visible absorption spectra of the glass with varying concentrations of TiO_2 and Au NPs. The absorption peaks were ascribed to the structural reposition of the glass due to the 4f–4f transition in erbium ions in the glass network [20]. Eight absorption peaks were positioned at different wavelengths of 411 nm, 446 nm, 487 nm, 521 nm,

545 nm, 653 nm, 798 nm, and 975 nm representing the transition of Er^{3+} ion from the ground state of $^4I_{15/2}$ to an excited state energy level of $^4F_{3/2}$, $^4F_{5/2}$, $^4F_{7/2}$, $^2H_{11/2}$, $^4S_{3/2}$, $^4F_{9/2}$, $^4I_{9/2}$, and $^4I_{11/2}$. Inset shows the physical appearance of TZNE, TZNETi, and TZNETiAu0.03 glass showing orangish nature [21] due to the contribution of Er^{3+} in Te-based glass stimulates a distinctive wavelength absorption in the visible spectrum [22]. Though, the incorporation of TiO_2 and Au NPs shows no changes in the color of the glass. According to Andreotti et al. [23], small sizes of NPs generate shielding properties of glass against ultraviolet light that cause the least degree of color changes.

At the fundamental absorption edge of crystalline and amorphous materials, there is the occurrence of two categories of optical transitions namely the direct and indirect optical transitions. Both the direct and indirect transitions occur due to the interactivity of electromagnetic waves with electrons that occupy the valence band elevated to the conduction band via the fundamental optical band gap. Figures 3b and 3c show the Tauc plot to determine the direct and indirect band gap. The linear region of $(\alpha\hbar\omega)^2$ as a function of $\hbar\omega$ and $(\alpha\hbar\omega)^{1/2}$ as a function of $\hbar\omega$ were extrapolated to satisfy the condition of $\hbar\omega$ at $(\alpha\hbar\omega)^2 = 0$ and $(\alpha\hbar\omega)^{1/2} = 0$ to estimate the direct (E_{dir}) and indirect (E_{indir}) band gap energies [2]. Urbach energy (E_U) can be used to assess the degree of disorder which is defined by the UV-Visible absorption data of the absorption coefficient and the corresponding energy [12]. Figure 3d illustrates a plot of ln (α) versus photon energy to determine the Urbach energy. The estimation of ΔE_U values was obtained from the reciprocals of the slopes of the plots of ln (α) versus $\hbar\omega$ [2].

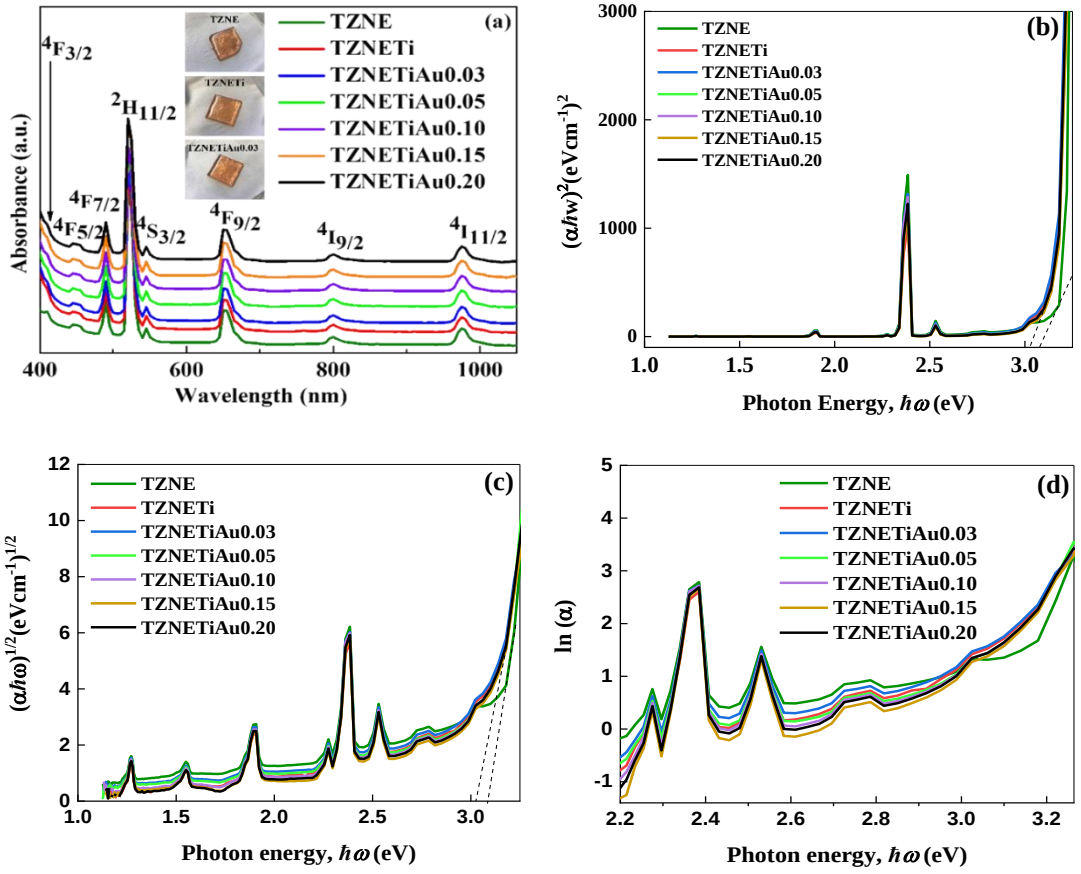

Fig. 3. (a) Absorbance spectra of glass (b) Tauc plot for direct band gap (c) Tauc plot for indirect band gap (d) Plot of ln α versus photon energy.

Figure 4a shows the value of direct and indirect band gaps with varying TiO_2/Au content. The direct and indirect band gap is discerned in the range of 3.185 – 3.211 eV and 3.049 – 3.138 eV, respectively. The first introduction of TiO_2 NPs into the glass (TZNETi glass) decreases the

band gap from 3.211 eV to 3.185 eV (for direct band gap) and from 3.138 eV to 3.049 eV (for indirect band gap), respectively. The decline in the optical band gap is a result of alteration in the local field around the Er^{3+} ions [11] that increases the number of NBO. The incorporation of NPs generates additional energy levels positioned in the gap of glass [24]. The incorporation of 0.03 mol% Au NPs increases the band gap from 3.185 eV to 3.197 eV (for direct band gap) and from 3.049 eV to 3.069 eV (for indirect band gap), respectively. The increase in the band gap signifies a reduction in the number of NBO or more BO being present [25].

However, further addition of Au NPs with a concentration of 0.05 mol% to 0.20 mol% shows a gradual decrement in the direct and indirect band gap signifies the increasing number of NBO. The generation of NBO opened the glass structure and facilitated the excitation of the electron because the electron exhibits a loose bond in NBO [26]. NBO atoms are present in the glass system. Nevertheless, the number of NBOs is elevated with the inclusion of Au NPs which makes the glass structure becomes less ordered. In addition, the inclusion of Au NPs into the glass matrix deteriorates the regular structure of glass and subsequently reduces the band gap [13]. Figure 4b illustrates the Urbach energy which lies in the range of 0.277 – 0.399 eV. The incorporation of TiO_2 and Au NPs up to 0.05 mol% elevated the Urbach energy. Upon the incorporation of bimetallic TiO_2 and Au NPs into the glass network, the disorder in the glass structure was elevated [11]. In the other studies conducted by Kolavekar et al. [2] and Zaini et al. [26], materials with higher impulses transform weak bonds into defects and display a higher value of Urbach energy. Variation in the direct band gap, indirect band gap, and Urbach energy is tabulated in Table 3.

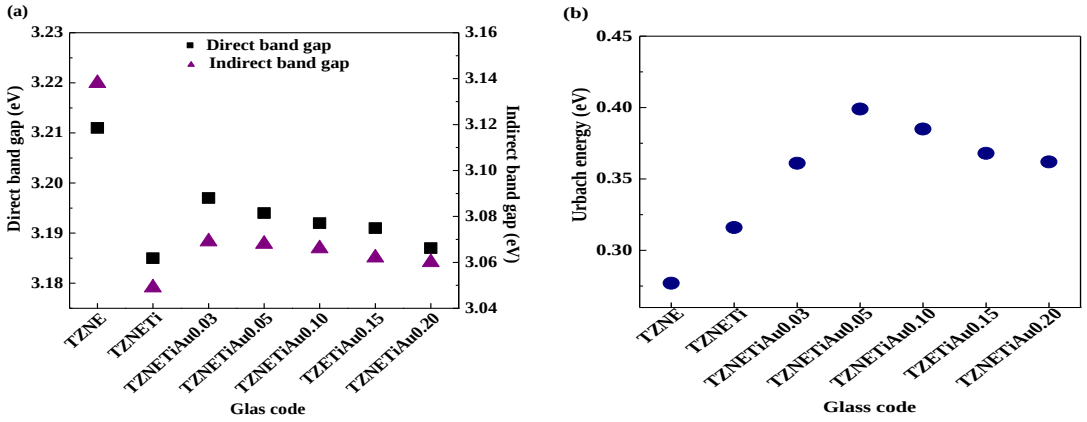

Fig. 4. Variation in the (a) direct and indirect band gap (b) Urbach energy.

Table 3. Optical band gap and Urbach energy of glass.

Optical properties	Glass Code						
	TZNE	TZNETi	TZNETiAu0.03	TZNETiAu0.05	TZNETiAu0.10	TZNETiAu0.15	TZNETiAu0.20
Direct band gap, E_{dir} (eV)	3.211	3.185	3.197	3.194	3.192	3.191	3.187
Indirect band gap, E_{indir} (eV)	3.138	3.049	3.069	3.068	3.066	3.062	3.060
Urbach energy, E_U (eV)	0.277	0.316	0.361	0.399	0.385	0.368	0.362

4. Conclusions

The direct incorporation of bimetallic TiO_2 and Au NPs into the glass matrix was demonstrated for the first time to tune the physical and optical traits of glass. The first introduction of TiO_2 NPs facilitates the generation of NBO which lowers the density (with a value from 5.200 $g.cm^{-3}$ to 5.166 $g.cm^{-3}$), increases the molar refractions (with a value from 15.836 cm^3 to 15.954 cm^3), elevates the refractive index (with a value from 2.343 eV to 2.349 eV), and reduces the direct band gap (with a value from 3.211 eV to 3.185 eV) and indirect band gap (with a value from of 3.138 eV to 3.049 eV). Meanwhile, the first introduction of Au NPs with a concentration of 0.03 mol% decreases the number of NBOs which increases the density (with a value from 5.166 $g.cm^{-3}$ to 5.189 $g.cm^{-3}$), decreases the molar refractions (with a value from 15.954 cm^3 to 15.865 cm^3), decreases the refractive index (with a value from 2.349 to 2.346), and elevates the direct band gap (with a value from 3.185 eV to 3.197 eV) and indirect band gap (with a value from 3.049 eV to 3.069 eV). Though, the addition of higher Au content of 0.05 mol% to 0.20 mol% causes further atoms rearrangement in the glass network.

Acknowledgements

The authors are thankful to the Ministry of Higher Education Malaysia (MoHE) and Universiti Malaysia Sabah for the financial support under the Fundamental Research Grant Scheme (vote FRGS/1/2019/STG02/UMS/02/1) and UMSGreat Grant Scheme (vote GUG0509-2/2020).

References

[1] T. Som, B. Karmakar, Nano Res. **2**, 607 (2009); https://doi.org/10.1007/s12274-009-9061-4
[2] S. B. Kolavekar, N. H. Ayachit, G. Jagannath, K. NagaKrishnakanth, S. V. Rao, Opt. Mat. **83**, 34 (2018); https://doi.org/10.1016/j.optmat.2018.05.083
[3] D. Sun, G. Zhang, J. Huang, H. Wang, Q. Li, Materials **7**, 1360 (2014); https://doi.org/10.3390/ma7021360
[4] S. K. Ghoshal, Asmahani Awang, M. R. Sahar, R. J. Amjad, M. R. Dousti, Chalcogenide Lett. **10**, 411 (2013).
[5] S.H. Alazoumi, S.A. Aziz, R. El-Mallawany, U.S. Aliyu, H.M. Kamari, M.H.M.M. Zaid, K.A. Matori, A. Ushah, Results in Physics **9**, 1371 (2018); https://doi.org/10.1016/j.rinp.2018.04.041
[6] C. Eevon, M.K. Halimah, M.N. Azlan, R. El-Mallawany, S.L. Hii, Mat. Sci-Pol. **37**, 517 (2019); https://doi.org/10.2478/msp-2019-0074
[7] R.J. Amjad, M.R. Sahar, M.R. Dousti, S.K. Ghoshal, M.N.A. Jamaludin, Opt. Express. **21** 14282 (2013); https://doi.org/10.1364/OE.21.014282
[8] A.S. Alqarni, R. Hussin, S.N. Alamri, S.K. Ghoshal, Journal of Taibah University for Science **14**, 954 (2020); https://doi.org/10.1080/16583655.2020.1791536
[9] B. Eraiah, Bull Mater Sci. **33**, 391 (2010); https://doi.org/10.1007/s12034-010-0059-z
[10] A.A. Ali, M.H. Shaaban, Silicon **10**, 1503 (2018); https://doi.org/10.1007/s12633-017-9633-y
[11] M. Azam, V. K. Rai, ACS Omega **4**, 16280 (2019); https://doi.org/10.1021/acsomega.9b00609
[12] R. Patwari D, B. Eraiah, J. Mat. Appl. **9**, 107 (2020); https://doi.org/10.32732/jma.2020.9.2.107
[13] M. K. Halimah, W. M. Daud, H. A. A. Sidek, A. W. Zaidan, A. S. Zainal, Mat. Sci-Pol. 28 (2010) 173–180.
[14] M. Elisa, R. C. Stefan, I. C. Vasiliu, S. M. Iordache, A-M. Iordache, B. A. Sava, L. Boroica, M. C. Dinca, A. V. Filip, A. C. Galca, C. Bartha, N. Iacob, M. I. Rusu, M. Eftimie, V. Kuncser, Nanomaterials **10**, 1875 (2020); https://doi.org/10.3390/nano10091875
[15] B. Eraiah, Bull. Mater. Sci. **29**, 375 (2006); https://doi.org/10.1007/BF02704138

[16] S. F. Ismail, M. R. Sahar, S. K. Ghoshal, Materials Characterization **111**, 177 (2016); https://doi.org/10.1016/j.matchar.2015.11.030
[17] W. L. Fong, K. A. Bashar, S. O. Baki, M. H. M. Zaid, B. T. Goh, M. A. Mahdi, J. Non-Cryst. Solids **555**, 120621 (2021); https://doi.org/10.1016/j.jnoncrysol.2020.120621
[18] M. K. Halimah, M. F. Faznny, M. N. Azlan, H. A. A. Sidek, Results in Physics **7**. 581 (2017); https://doi.org/10.1016/j.rinp.2017.01.014
[19] R. P. V. Duyne, J. C. Hulteen, D. A. Treichel, J. Chem. Phys. **99**, 2101 (1993); https://doi.org/10.1063/1.465276
[20] N.N.A. Razali, I.S. Mustafa, N.Z.N. Azman, H.M. Kamari, A.A. Rahman, K. Rosli, N.S. Taib, N.A. Tajuddin, J. Phys.: Conf. Ser. **1083**, 012004 (2018); https://doi.org/10.1088/1742-6596/1083/1/012004
[21] I. Ferodolin, A. Awang, S.K. Ghoshal, A. Samavati, C.F. Pien, J. Dayou, J. Lumin. **241**, 118488 (2022); https://doi.org/10.1016/j.jlumin.2021.118488
[22] R. El-Mallawany, M.D. Abdalla, I.A. Ahmed, Mater. Chem. Phys. **109**, 291 (2008); https://doi.org/10.1016/j.matchemphys.2007.11.040
[23] A. Andreotti, M. Goiato, A. Moreno, A. Nobrega, A. Pesqueira, D. Santos, Int. J. Nanomedicine. **9**, 5779 (2014); https://doi.org/10.2147/IJN.S71533
[24] H. Aboud, J. Nanostruct. **6**, 179 (2016); https://doi.org/10.7508/JNS.2016.03.001
[25] N. Elkhoshkhany, S. Marzouk, M. El-Sherbiny, H. Ibrahim, B. Burtan-Gwizdala, M. S. Alqahtani, K. I. Hussien, M. Reben, E. s. Yousef, Materials **15**, 5393 (2022); https://doi.org/10.3390/ma15155393
[26] N. A. Zaini, S. N. Mohamed, Z. Mohamed, Materials **14**, 3710 (2021); https://doi.org/10.3390/ma14133710